Hydrogenolysis of 5-Hydroxymethylfurfural To Produce 2,5- Dimethylfuran over ZrO_2 Supported Cu and RuCu Catalysts

Jesús M. Requies, Mikel Frias, Marcos Cuezva, Aitziber Iriondo, Ion Agirre, Nerea Viar.

Chemical and Environmental Engineering Department, Engineering Faculty of Bilbao, University of the Basque Country (UPV/EHU), C/Plaza Ingeniero Torres Quevedo 1, 48013 Bilbao, Spain

ABSTRACT: Glucose dehydration to HMF and its hydro- genolysis to DMF, a suitable biofuel, have been studied using the same catalysts for both processes. The 10CuZr catalyst shows the highest HMF yield (25.6%) with an acceptable glucose conversion (75.8%) after 1.5 h on stream. By increasing the time on stream from 1.5 to 5.5 h the HMF yield (33.2%) and glucose conversion (94.5%) are improved. In the case of DMF production, the 15CuZr catalyst shows the highest DMF yield (30%). This behavior is notably improved when Ru is added to the 15CuZr catalyst, reaching a DMF yield of 45.6%. These activity results could be related to the higher amount of Cu^0 species exposed on the catalyst surface and the increase of coke resistance. Finally, the 1Ru15CuZr catalyst is used in DMF production using glucose derived HMF as raw material, and a DMF yield and HMF conversion of 16.4% and 77.5% are achieved, respectively.

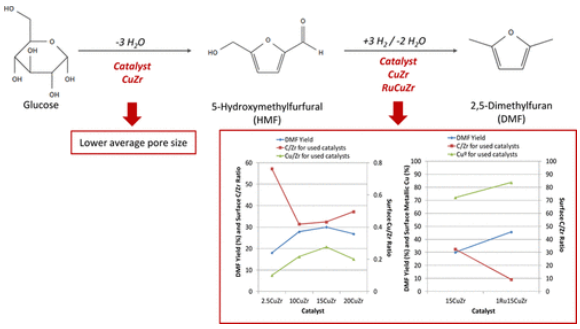

1. Introduction

Petroleum, coal, and natural gas still represent the most important resources in the current energy system, 80% of the primary energy consumption.[1,2] The oil production increases year by year, and the carbon proportion in the world electricity mix has increased in the last years.[3,4] However, these energy sources are fossil fuels, and there are serious concerns about their depletion in the following decades.[2,5–7] Apart from all these data, there is evidence that the climate of the planet is changing due to the global warning. The temperature of the earth is increasing, and the ice of the poles is beginning to melt; all these changes are attributed to the Greenhouse Effect produced by the CO_2 emissions coming from the combustion of fossil fuels.[5,8]

Petroleum not only plays an important role in the transportation sector, where the main fuels and additives have a nonrenewable petroleum-derived origin, but also in the chemical industry. It must be taken into account that some oil- derived chemicals are the base or platform products in the production of a wide variety of products like plastics, carpets, cloths, wall paints, perfumes, hairsprays, etc.[9] Thus, research and development in sustainable and environmentally friendly alternatives has become one of the technological goals of the near future.

The biorefinery can be a good alternative to cover the current needs of energy, fine chemicals, and unconventional fuels.[1,10] Regarding biodiesel and bioethanol generated from first generation biomass, it must be said that they had a great contribution on the transportation sector, but they came into conflict with the food industry.[11,12] Moreover, due to the drawbacks presented by this first generation biofuels in their use in transportation motors, the efforts are leading to the development of second generation biofuels and bioadditives,[11,13] which can be produced from nonfood residual lignocellulosic biomass (sugars).[7,12,13]

According to the literature,[14] the top seven chemical building blocks can be produced from sugars using a chemical route: levulinic acid, glucaric acid, sorbitol, arabitol, xylitol, furfural, and 5-hydroxymethylfurfural (HMF). HMF is an aromatic aldehyde, and it is believed as an outstanding platform chemical due to its many advantages. It is considered as a bridge between biomass resources and biochemicals.[15] HMF production has the great advantage that it can be produced from different sugars like glucose, fructose, and sucrose, and afterward, it can be converted into biofuels, such as 2,5-dimethylfuran (DMF), and some other fine chemical molecules like levulinic acid (LA), 2,5-furandicarboxylic acid (FDCA), or ethyl levulinate (EL).[1,6,10,15−17] The present paper focuses on the use of lignocellulosic biomass in the production of HMF and its posterior conversion into DMF.

HMF used to be separated from the reaction mixture of fructose, sucrose, and oxalic acid.[17] Nowadays, the most extended reaction to produce HMF is dehydration of the aforementioned carbohydrates over acid, homogeneous, or heterogeneous catalysts.[1,10,16,17] The most used carbohydrate is fructose rather than glucose and sucrose due to its higher reactivity toward HMF. However, in the last years the research is focused on the use of glucose, which can be obtained from cellulose hydrolysis, as raw material for HMF production.[18−21] DMF is considered as a high-quality fuel, as ethanol, an ideal renewable and sustainable substitute or additive of conventional gasoline.[2,15] It presents a high energy density, similar to that of gasoline and higher than ethanol,[6,13] and high octane number, higher than gasoline.[1] Moreover, DMF shows very low solubility in water, and therefore it can be used as a blender in transportation fuels.[13,22] In this sense, some literature reports the good performance of the DMF as a fuel on direct injection spark ignition (DISI) type engines[6,8] without any important modifications of the engine and also in compression engines.[23] Other authors like Jezak et al.[24] conclude that DMF could be an additive to petroleum-based fuels but taking into consideration pressure and temperature conditions. Moreover, DMF reduces significantly the amount of large particles produced, reducing the total mass of particles emitted, although it is not able to reduce significantly the number of particles smaller than 10 nm.[25] DMF can be produced from hydrogenolysis, also called selective hydrogenation, of HMF[13] using non-noble and noble metal catalysts according to the last findings published recently in the open literature.[1,2] This reaction involves different pathways[1,13,26] in which dehydration and hydrogenation reactions are predominant. Figure 1 shows a simplified reaction scheme of DMF production from biomass.

As reported in the recent literature about this topic, DMF production from HMF catalytic hydrogenolysis is mainly carried out by batch systems,[1,6,16,22,26,31] using synthetic HMF as reactant and noble, such as Pd, Pt, Ru, Rh, and Au,[1,2,22,31−33] and non-noble, such as Cu, Co, Ni, and Fe,[6,34,35] metal-based catalysts. Only a few research works report information about hydrogenolysis of HMF over continuous systems[10,33,36] using real feed of HMF.[11,16,36]

Based on this background and the results obtained in our previous research,[11] which concluded that the neutral nature supports, such as ZrO_2, seem to be promising materials, the present work deals with the production of DMF (via HMF) using synthetic glucose as feedstock using a continuous reactor and different Cu/ZrO_2 catalysts. In order to achieve this objective, the experiments were carried out in two steps:

I. HMF production from glucose in a batch reactor. The obtained HMF was denoted “low grade HMF”.

II. Conversion of HMF into DMF in a continuous fix bed catalytic reactor. This second step was carried out also in two different steps:

II.a) Optimization of reaction conditions using syn- thetic HMF, which was named “high grade HMF”.

II.b) DMF production from “low grade HMF.

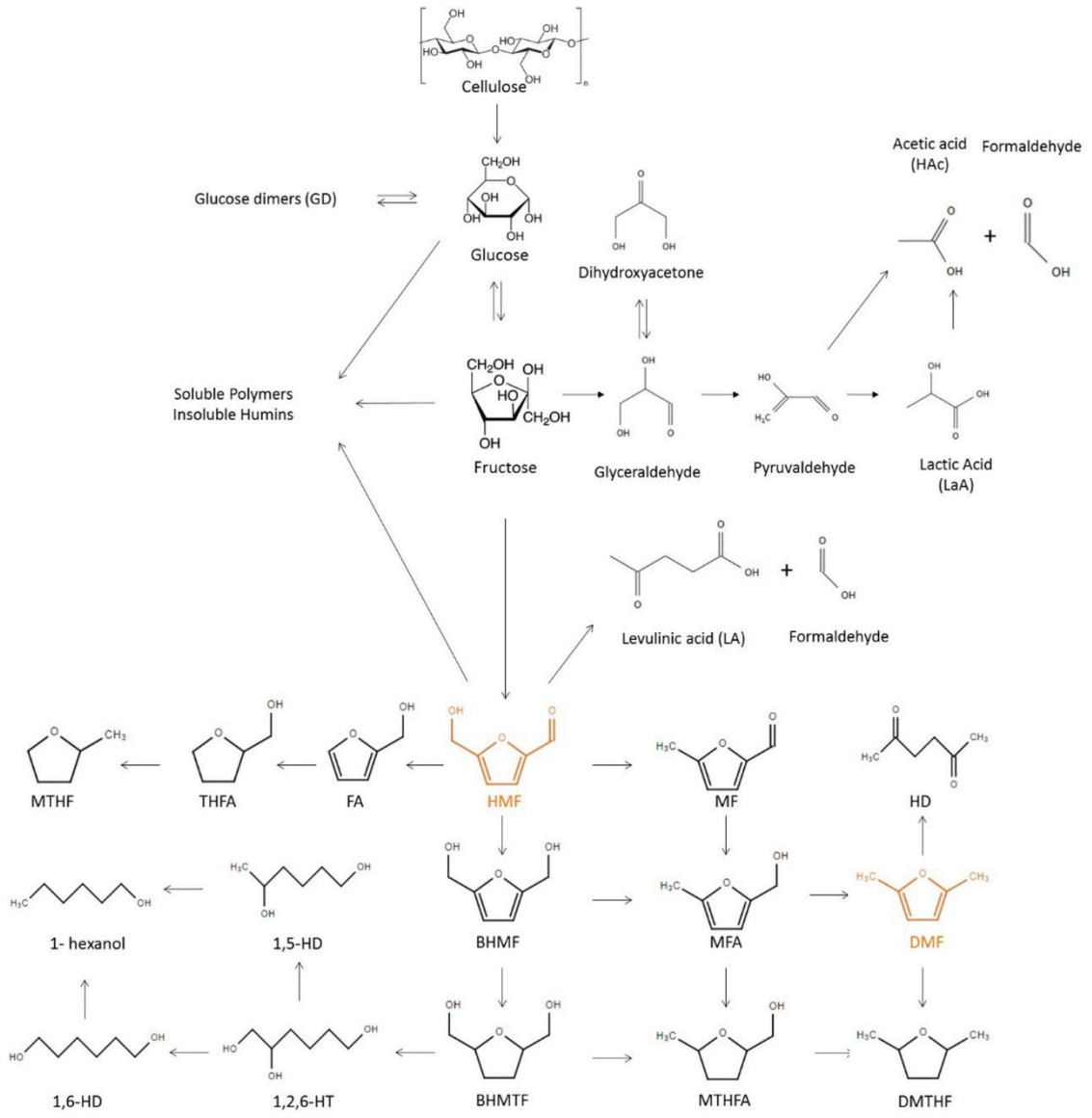

Figure 1. Desirable production route of DMF via HMF from biomass. Adapted from refs 11, 18−21, and 27−30.

2. Experimental procedure

2.1. HMF and DMF production

Synthetic glucose (Sigma-Aldrich, ≥99%) was used to produce “low grade HMF”. Different supports and catalysts were tested using a stirred 50 mL autoclave reactor where the temperature is controlled by an external thermocouple placed inside the reaction mixture. Single-phase and biphasic reactor systems were studied adding different quantities of 1-butanol (Sigma- Aldrich, ≥99%) into the aqueous reactant mixture. 1-Butanol is one of the most used polar protic solvent agents in DMF

production.[16,22,31,36] However, some other supercritical com- pounds and ionic liquids are also used as solvents as report Bhanja and Bhaumik in their review article.[37] Once the reactant solution (2.5 wt % of glucose, 26 wt % of water, and 71.5 wt % of 1-butanol) was incorporated into the batch reactor, the production of HMF was carried out under 1.5 MPa of N_2 and 200 °C. The reactor was maintained under these conditions during a certain period of time, in which it was not possible to withdraw samples, and after it the reactor was cooled down, and the reaction products were analyzed by GC-FID and HPLC.

In order to produce DMF "high grade HMF" (Sigma- Aldrich, 99%) diluted in 1-butanol was used as a first step. For this purpose a continuous bench-scale fixed bed reactor in which 0.5 g of catalyst was diluted with inert SiC (catalyst/SiC= 1:9 wt), corresponding to WHSV (g HMF/(g cat·h)), a value of 0.15 h^{-1} was used. Prior to the hydrogenolysis reaction, all tested catalysts were activated in situ under 100 N mL/min of H_2 at 0.1 MPa and 400 °C for 2 h. The activity tests were carried out at 200 °C and 15 bar of H_2. The feed and output liquid streams were collected and analyzed by an HPLC and by GC-FID. After the optimization of the DMF production process using "high grade HMF", the "low grade HMF" was used as feed in this second step.

For a better understanding of catalytic activity and product distribution, parameters such as glucose conversion and HMF yield (%) in the first step and HMF conversion (%) and DMF yield (%) are used in this work:

$$Conversion\ (\%) = \frac{N^{in}_{glucose/HMF}(mol/min) - N^{out}_{glucose/HMF}(mol/min)}{N^{in}_{glucose/HMF}(mol/min)} x100$$

$$Yield\ (\%) = \frac{N^{out}_{HMF/DMF}(mol/min)}{N^{in}_{glucose/HMF}(mol/min)} x100$$

2.2. Analysis.

Both the reactants (glucose and HMF) and the reaction products (HMF and DMF) were analyzed by chromatography. HMF quantity on feed and liquid product stream was analyzed by an Agilent HPLC chromatograph (1260 Infinity) equipped with Hi-Plex H column and infrared detector; DMF and other products in the liquid product stream were quantified using a Hewlet Packard GC using a flame ionization detector (FID) equipped with a Suprawax 280 capillary column.

2.3. Catalyst preparation.

For these experiments Cu and Ru−Cu catalysts supported on commercial ZrO_2 (Alfa Aesar, ZrO_2 99%), designed as ZrO_2, were prepared by the wetness impregnation method. $RuCl_3$ (Johnson Matthey, metallic base Ru 40%) and $Cu(NO_3)_2{\cdot}3H_2O$ (Alfa Aesar, 98%) salts were used as ruthenium and copper precursors, respectively. The monometallic Cu catalysts, designed as 2.5CuZr, 10CuZr, 15CuZr, and 20CuZr in which the numerical factor belongs to nominal wt % of copper, were prepared by a single step impregnation. Conversely the bimetallic catalyst, designed as 1Ru15CuZr (also in nominal weight), was carried out by impregnation of the 15CuZr catalyst with a ruthenium precursor solution. After impregnation and drying, the samples, including ZrO_2 support designed as ZrO_2 cal, were calcined in air at 250 °C for 2 h.

2.4. Catalyst characterization.

The catalysts were characterized by several physicochemical techniques such as plasma atomic emission spectroscopy (ICP-AES), surface area (BET method), temperature-programmed reduction (TPR),

temperature-programmed desorption with ammonia (TPD), in order to measure the acidity of the catalysts, X-ray photo- electron spectroscopy (XPS), CO chemisorption (CO-TPD), and transmission electron microscopy (TEM).

2.4.1. Plasma Atomic Emission Spectroscopy

Metal contents were determined by ICP-AES, using a PerkinElmer Optima 3300DV apparatus, previous dissolution of the ground samples in acid solutions (37.5% HNO_3, 37.5% HF, and 25% HCl, in volume).

2.4.2. Textural properties.

BET surface area and pore characteristics of the calcined fresh catalysts were evaluated from the N_2 adsorption−desorption isotherms obtained at −198 °C over the whole range of relative pressures. In the case of the CuZr, RuCuZr, and Zr catalysts, these samples were characterized using Autosorb-1-C/TCD (Quantachrome, USA) after outgassing solid samples at 150 °C for 24 h. Average pore sizes were determined by using the BJH method

2.4.3. H_2-TPR analysis

This technique was used to study the reducibility of the calcined catalysts. The measurements were carried out using an AutoChem II Instrument (Micro- meritics, USA) equipped with a TCD detector. TPR profiles were obtained by heating the samples from room temperature to 900 °C at a linearly programmed rate of 10 °C/min, while 50 mL/min of reduction gas (5% v/v H_2 diluted in Ar) was passed through the sample. The temperature was increased from room temperature to 1000 °C at a rate of 10 C/min. The samples were previously outgassed at 200 °C for 30 min.

2.4.4. X-ray photoelectron spectroscopy (XPS)

This technique was used to evaluate the surface characteristics (oxidation state of the species formed, interactions, atomic ratios, etc.) of the samples. The measurements were carried out with a VG Escalab 200R spectrometer equipped with a hemispherical electron analyzer and an Al K1 (h = 1486.6 eV) 120W X-ray source. The powdered samples were deposited on a stainless steel sample holder, placed in the pretreatment chamber, and degassed at 300 °C. The spectrometer base pressure was typically 10−9 Torr (0.00133 MPa). The spectra were collected at a pass energy of 20 eV, which is typical of high resolution conditions. Both fresh and spent catalysts were analyzed with this technique.

2.4.5. Temperature-programmed desorption with ammonia (NH_3-TPD)

Temperature-programmed desorption of NH_3 was used in order to know the acid characteristics of the calcined samples. The used equipment was an AutoChem II instrument. First of all, samples were flushed by He at 250 °C for 30 min, followed by a reduction step with a 5%H_2/He mixture, followed by a cooling step at 40 °C, and loading of NH_3 for 30 min. Then the physically absorbed NH_3 was removed using He at 85 °C until no further desorption was recorded. Finally, the release of chemically adsorbed NH_3 was collected increasing temperature from 85 to 800 °C at a rate of 10 °C/min. The samples were previously outgassed at 200 °C for 30 min

2.4.6. Transmission electron spectroscopy analysis

TEM work was performed on a Philips SuperTwin CM200 operated at 200 kV and equipped with LaB6 filament and an EDAX EDS microanalysis system. The samples for the fresh-reduced TEM were prepared by dispersion into isopropyl alcohol solvent and keeping the suspension in an ultrasonic bath for 15 min, after a drop of suspension was spread onto a TEM Ni grid (300 mesh) covered by a holey carbon film followed by drying under vacuum.

2.4.7. Temperature-programmed desorption with CO (CO-TPD)

Temperature-programmed desorption of CO was used in order to know the dispersion of the fresh reduced catalysts. The used equipment was AutoChem II instrument. First of all, samples were reduced by a 5%H_2/He mixture at 523 K for 60 min, followed by a cooling step at 313 K, and loading of CO in different pulses of CO for 30 min. The samples were previously outgassed at 200 °C for 30 min. 2.4.8. Diffuse reflectance infrared fourier transform (DRIFT) Diffuse reflectance infrared Fourier transform, DRIFT, was used to distinguish Lewis and Brönsted acid sites of the catalysts under study in the present paper. A VERTEX 70 spectrometer coupled with an external sample chamber that enables measurements under vacuum and a mercury cadmium telluride (MCT) detector was used (Bruker, Germany). The samples were pretreated in situ under vacuum for 1 h at 250 °C and later cooled down to 40 °C in order to record the background spectra. The main measurement features were a spectral range from 1800 to 1200 cm^{-1}, 200 scans, and a resolution of 4 cm^{-1}. After the pretreatment, the catalysts were kept in contact with pyridine vapor at 40 °C for 15 min. Afterward measurements were carried out at 40 °C after heating the sample up to 150 and 200 °C (reaction temperature), for 15 min, respectively.

3. Results and discussion

3.1. Catalyst characterization results

3.1.1. Chemical and textural properties

The nomenclature of the different prepared catalysts, their real copper and ruthenium contents determined by ICP-AES, and values of the textural properties are presented in Table 1. It can be observed that all of the prepared catalyst show a chemical composition close to the theorical one. With regards to the surface are and pore volume, the commercial Zr support presents low surface area and pore volume. Moreover, when the copper is added to the support, the surface area is even lower for all the prepared catalysts, indicating that copper species are preferentially deposited in the pore structure of the support.

The incorporation of the lowest quantity of copper slightly reduces the pore volume of the catalyst, but when the higher copper amounts are added, this value falls down significantly. These results could be related to the progressive increase of metal content, with the 20CuZr exception, which produces the blocking of smallest pores and ends blocking the largest ones.[38]

The incorporation of a small quantity of ruthenium to the 15CuZr catalyst does not influence neither on the surface area nor in the pore volume since the values are quite similar. The data presented for average pore size parameter corroborate that the 15CuZr catalyst shows a higher average pore size than the calcined support, suggesting that pore size distribution is moving to larger pore size because of the filling of the smallest pores.[39] However, the rest of the catalysts present lower pore size than the support, reaching the lowest average pore size for the 10CuZr catalyst.

Table 1. Nomenclature, Metal Loading, and Textural Properties for Calcined Pure Support and Cu and RuCu Catalysts

Catalyst	Metal content		S_{BET}	Pore volume	Av pore size
	Cu (%)	Ru (%)	(m^2/g)	(cm^3/g)	(nm)
ZrO_2 cal[a]			15	0.0125	3.66
2.5CuZr	3		12	0.0110	3.15
10CuZr	11		10.5	0.0083	3.13
15CuZr	17		9.4	0.0074	3.71
20CuZr	23		9.6	0.0078	3.20

1Ru15CuZr	17	1	9.5	0.0076	3.25

[a]cal = calcined

3.1.2. Reducibility

The calcined catalysts were characterized by the TPR technique, and the obtained profiles are shown in Figure 2, except for the case of the 2.5CuZr catalyst, which did not present any reduction peak. This observation could be due to the low amount of Cu, which strongly interacts with the support.[40] The reduction profiles suggest that all of the catalysts show a broad reduction range in which peaks are overlapped. Concretely, the supported Cu catalysts present the highest reduction peak in the temperature range that goes from 100 °C to around 300 °C, and they present another peak between 300 and 550 °C. According to the literature[11,41] this observation suggests the presence of CuO_x species with different interaction with the support. Concretely, species detected at low temperature range are ascribed to heterogeneous distributed well dispersed CuO species, while peaks registered at a higher temperature range are associated with bulk or strongly Cu species interacting with the support.[41−43] Although the 15CuZr and 1Ru15CuZr catalyst's deconvolution profiles are only presented as examples (Figure 3), all supported Cu catalysts show a contribution of two peaks for the lowest temperature peak. This fact could be suggested that a contribution of sequential reduction of CuO species from Cu^{2+} to Cu^{1+} and from Cu^{1+} to Cu^{0} [11] of non-uniform distributed Cu species.[44,45] On the other hand, those Cu species that strongly interact with the support seem to be more important for the 15CuZr catalyst than for the rest of the Cu catalysts.

When Ru is added to the 15CuZr catalyst, reduction peaks are moved to lower temperatures (below 300 °C), which indicates that the presence of Ru improves the Cu reduction capacity and modifies the interaction of Cu with the support. When $RuCl_3$ is used as the precursor salt, an interaction between support and the metallic salt is generated.[46] This interaction among the precursor salts can modify the metal's reduction; in this case it was observed a shift in reduction temperature that may be caused by interphase hydrogen adsorption, which favors Cu reduction.46 However, the improvement in Cu reducibility could be also due to the presence of a second noble metal47−49 which facilitates the spillover from Ru atoms. Moreover, as Figure 3 indicates, the detected reduction peak presents a contribution of reduction of Cu species, as explained above, and reduction of Ru species. In this last case, according to the literature,50 the Ru species correspond to well dispersed RuO_x and RuO_2.

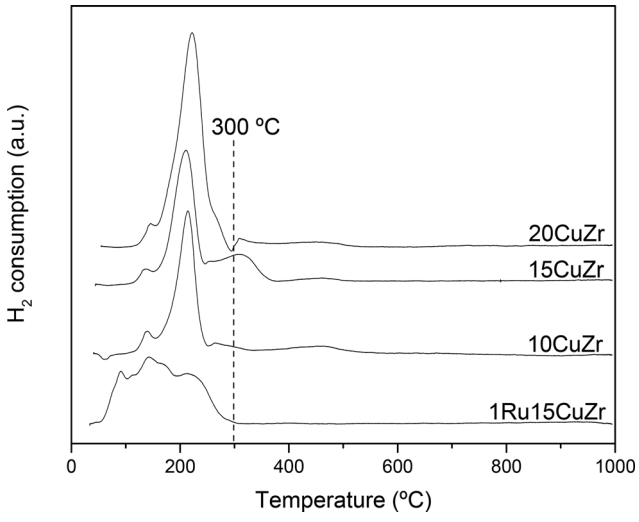

Figure 2. TPR profiles of the ZrO_2 supported Cu and RuCu catalysts

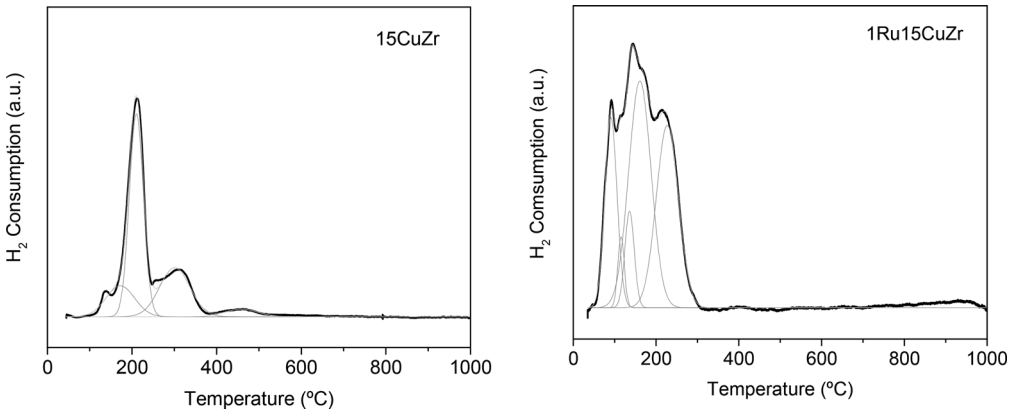

Figure 3. Deconvolution of 15CuZr and 1Ru15CuZr catalysts profiles

3.1.3. Acidic properties

Acidic properties of the catalyst, which are determined by the TPD-NH_3 characterization technique, play an important role in dehydration of glucose to HMF. On the other hand, it is important to understand these characteristics because a very acid catalyst could cause the HMF ring opening, reducing DMF yield. TPD-NH_3 profiles of the prepared samples are included in Figure 4, and total acidity is reflected in Table 2.

With regards to the acid properties of the catalysts, the NH_3 desorption temperature indicates the acid sites strength on the catalytic surface. In this sense, the desorption signals lowerthan 200 °C, between 200 and 450 °C, and higher than 450°C are attributed to weak, medium, and strong acid sites, respectively. As Figure 4 shows, the pure and calcined ZrO_2 supports present mainly low-weak acidic sites, with a total amount of desorbed NH_3 of 0.08 and 0.09 mmol of NH_3/g of catalyst (see Table 2), respectively. Supports present a similar NH_3 desorption profile, but the calcined one presents a little bit more acidity than the fresh one. Some authors explain that this slight difference between the two supports is probably due to the presence of zirconium sites acting as Lewis acid sites besides the formation of H^+ as a Brönsted acid from the calcination processes[51] and/or due to the change of the ZrO_2 phase.[52] The acidity of the ZrO_2 is slightly changed when the fraction of the tetragonal phase is increased,[53] and this phase change occurs when the calcination temperature is maintained at 450 °C during different times. The FTIR results indicate (see Figure S3) that there are not Brönsted sites; therefore, the higher acidity of the calcined support may be due to the change of the ZrO_2 phase.

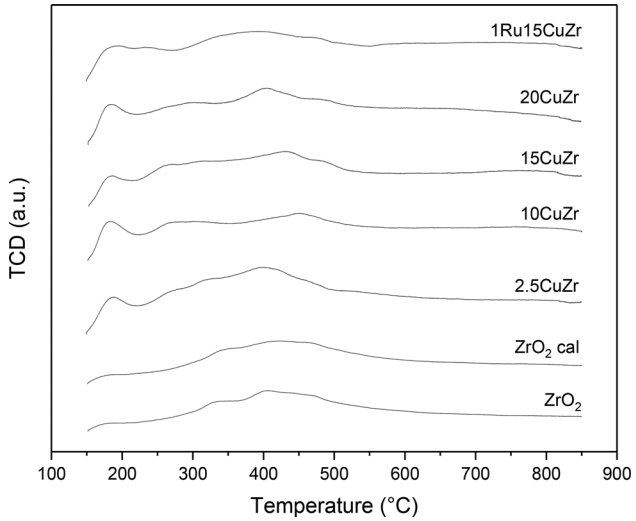

Figure 4. NH_3-TPD profiles of pure support and Cu and CuRu catalysts

Table 2. Results obtained from NH_3-TPD and TEM characterization techniques for pure support and Cu and CuRu catalysts

Catalyst	mmol NH_3/g_{cat}[b]	Cu particle size (nm) [c]		Ru particle size (nm)[c]
		dp internal	av dp	
ZrO_2	0.08			
ZrO_2 cal[a]	0.09			
2.5CuZr	0.15			
10CuZr	0.13	< 1500	500-700	
15CuZr	0.14	100-1000	500-700	
20CuZr	0.15	100-1000	300-400	
1Ru15CuZr	0.14	100-1000	500-700	5-10

[a]cal = calcined

It can be also observed in Table 2 that the incorporation of Cu to the calcined support increases the total acidity of the catalysts. This behavior could be due to the formation of copper crystallites on oxide form.[40,54] However, the acidity keeps almost constant when Cu loading is increased. Chary et al.[55] suggest that the increment in the copper crystallinity may provide more surface available for dehydration activity. This crystallinity was observed in the high crystal size of the copper determinated by TEM and CO chemisorption analyses; this high crystallinity is related to the high particle size of the Cu particles (more than 500 nm as it is presented in Table 2). Moreover, a slight difference in the acidity strength was observed for Zr-supported Cu catalysts, whose TPD-NH_3 profiles present an additional peak at 200 °C, indicating the aforementioned formation of additional acidity. Nevertheless, this new peak is located in the range of the lowest acid strength.

The addition of Ru to 15CuZr catalyst has no significant effect on the acidity of the catalyst (see Figure 4 and Table 2).

FTIR measurements were also performed in order to analyze the Lewis/Brönstend acid sites ratio (see Figures S3 and S4). The main conclusions of these analyses were that all the acidity of ZrO_2 support and CuZr and RuCuZr catalysts was due to the Lewis acid sites, being that these acid sites are weak and medium. As it is previously mentioned, the support calcination can create Brönsted acid sites, but according to Lee et al., temperatures around 600 °C are required to create these Brönsted acid sites;[56] in the present case, the calcination temperature was 250 °C; therefore, no Brönsted acid sites were expected to be formed during the calcination process. FTIR profiles, which were registered at 40, 80, 150, and 200 °C, suggest that all of the prepared catalyst samples present only very low intensity peaks associated with Lewis acid sites. Concretely at the highest temperature (the reaction temper- ature), at 200 °C, no peak of acid Lewis sites was detected. These results, together with ammonia TPD measurements, are indicative that these catalysts present low acidity strength.

3.1.4. Surface properties

Surface properties, such as surface atomic ratios and amount of different species, obtained from the XPS characterization technique, are reflected in Table 3. As it is observed, the Cu/Zr surface atomic ratio of fresh reduced monometallic catalysts increases when more Cu is added. However, this improvement is not detected when Cu loading is increased from 15 to 20 wt %, being the Cu/Zr atomic ratio value of 0.408 for both 15CuZr and 20CuZr catalysts. This fact could suggest that Cu species probably also suffer from

sintering phenomena.

The Cu/Zr bulk ratio was also determined in order to compare to Cu/Zr measured by XPS. It can be observed that all the catalysts, except for the 20CuZr catalyst, present a higher ratio than the bulk one. This fact indicates that all the copper was incorporated on the surface of ZrO_2 support. This is a good agreement with the TEM and BET results.

In the case of the fresh reduced 1Ru15CuZr catalyst, an increase of Cu/Zr surface atomic ratio is observed when compared with its monometallic counterpart, indicating that the number of Cu species exposed on the surface is increased. As it is aforementioned, the addition of a low amount of a noble metal leads also to a higher metal dispersion, and therefore a higher metallic surface area, and a higher reduction degree, as the TPR profile of 1Ru15CuZr suggests. According to the literature,[49,57] the presence of a noble metal to a non- noble monometallic catalyst seems to generate an intimate contact and a synergy effect between both metals, resulting in a better surface exposure, reduction capacity, metal dispersion, and metal surface area.

The detected Cu species on the exposed surface are Cu^0, Cu^+, and Cu^{2+}, being the predominant metallic one on the fresh reduced catalysts, except for 2.5CuZr and bimetallic catalysts. According to the literature,[58] Cu^0 and Cu^+ have the same Cu 2p binding energy (932.6 eV) but different CuLMM peaks, 225.0 and 337.4 eV, respectively. Taking into account this fact, the CuLMM binding energy was also analyzed in order to register the presence of the two copper phases in all fresh-reduced and used catalysts (see Figure S1). However, when the monometallic and bimetallic catalysts are used in the HMF hydrogenolysis, the surface exposure of Cu species decreases in all of the cases, and the Cu^0 species suffer an oxidation phenomenon, resulting in a lower $Cu^0/(Cu^{2+} + Cu^+)$ ratio than when compared with fresh reduced catalysts. This last observation (see Figure S1) did not happen in the bimetallic catalyst, for which the $Cu^0/(Cu^{2+} + Cu^+)$ ratio increased after its use in the reaction. This fact could be related to the better reducibility of the 15CuZr catalyst improved by the Ru presence, corroborated with the TPR profiles. Moreover, this reduction capacity can be related with the lowest amount of coke on the catalytic surface. It seems that the incorporation of the little amount of Ru on the catalysts, whose dispersion remained almost constant after reaction (see Table 3), improves the metal reduction during the reaction, improving the stability of the catalysts and limiting the coke formation,[59,60] as the C/Zr ratio suggests. Unlike the 1Ru15CuZr catalyst, the use of Cu-supported catalysts in the hydrogenolysis reaction provokes the formation of great quantities of coke.

Table 3. Results of surface atomic ratios and qualitative proportion of different species determined by XPS characterization technique[a]

Catalyst	Cu/Zr	Cu/Zr_{ICP}	Ru/Zr	$Cu^0/(Cu^+ + Cu^{2+})$	C/Zr
2.5 CuZr	**0.235**	**0.043**		**40/62**	**1.40**
	0.101			38/62	57.20
10CuZr	**0.280**	**0.175**		**70/30**	**1.21**
	0.216			60/40	31.4
15CuZr	**0.408**	**0.303**		**69.8/30.2**	**1.37**
	0.277			67/33	32.4
20CuZr	**0.408**	**0.505**		**74/26**	**1.37**
	0.201			47.5/52.5	38.2

	1.400	**0.310**	**0.047**	**27.5/72.5**	**3.70**
1Ru15CuZr					
	0.190		0.045	51.4/48.6	9.20

[a] Bold text: fresh reduced catalyst; non bold text; catalysts in HMF hydrogenolysis

3.1.5. Morphological characteristics

Derived results of TEM measurements, which were performed with fresh reduced catalysts, are reported in Table 2 and Figure 5. Black color represents the copper particles, and the more transparent particles correspond to the ZrO_2 particles. In the case of the 1Ru15CuZr catalyst, the ruthenium particles are also in black color. The identification of the different species was developed by energy dispersive spectroscopy. In Figure 5, it can be observed large copper particles indicating that Cu dispersion on ZrO_2 is very low. In fact, it is possible that the zirconia can be dispersed on copper.

Most of the TEM pictures show that the Cu particles present a large particles size (1000−1500 nm), being the average particle size around 400−500 nm, while the ZrO_2 particle size is around 30−60 nm. Therefore, as aforemen- tioned, it seems that instead of having Cu dispersed on ZrO_2, it is ZrO_2 which is dispersed on Cu. The 20CuZr catalyst shows some areas with sintered ZrO_2 and no Cu. This evidence is even more evident with the 2.5CuZr catalyst, where some pictures show only Cu but most of them show the presence of sintered ZrO_2 particles without any Cu particle; this behavior could explain the nonexisting reduction peak observed in TPR for the 2.5 CuZr catalyst. Concerning the 1Ru15CuZr catalyst, similar Cu and ZrO_2 particle sizes are observed. However, in this case, Ru is well dispersed with particle size of 5−10 nm. The ruthenium particles are spheres, and they are dispersed on the ZrO_2 as well as on the copper particles.

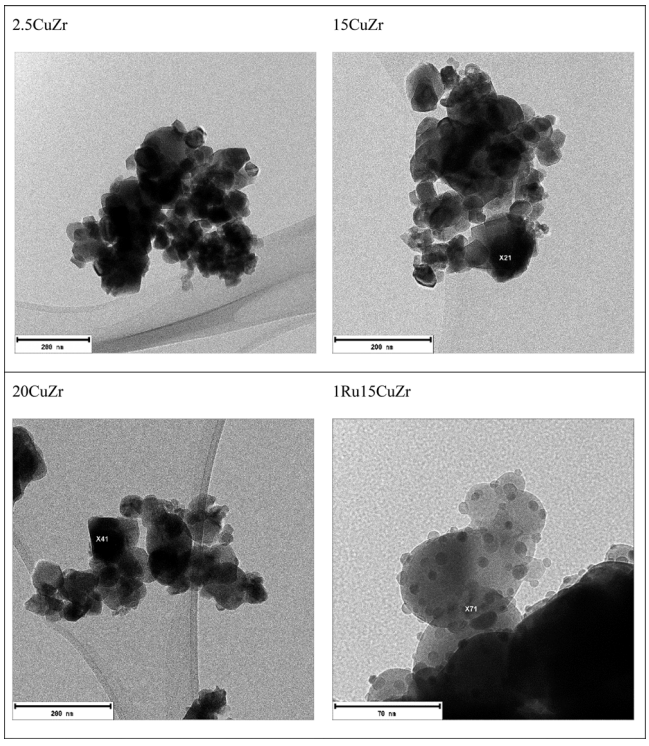

Figure 5. TEM images of fresh reduced 2.5CuZr, 15CuZr, 20CuZr and 1Ru15CuZr catalysts

Complementary to TEM pictures CO chemisorption was performed to determinate the copper dispersion. As it can be observed in Table S1, the determined metal dispersion by CO chemisorption for the fresh-reduced catalysts was very low, as it was also observed by TEM. All the catalysts present a metal dispersion lower than 1%. The metallic surface area was also very low for all the catalysts due to the high metal particle size. The 1Ru15CuZr catalysts reached the highest metallic surface area. This catalyst

presents more metallic dispersion than the monometallic 15CuZr catalyst. This effect could be corroborated by the aforementioned XPS results. Thus, the presence of a noble metal to a non-noble monometallic catalyst seems to generate an intimate contact and a synergy effect between both metals, resulting in a better surface exposure, reduction capacity, metal dispersion, and a higher metal surface area. Regarding the monometallic catalysts, all of them present similar metallic surface areas, following this order: 2.5CuZr, 15CuZr, 10CuZr, and 20CuZr.

3.2. Activity results

Two activity tests were carried out: (i) dehydration of glucose to produce HMF and (ii) the hydrogenolysis of HMF to produce DMF.

3.2.1. HMF production

Aqueous (10 wt % of glucose and 90 wt % of water), organic (10 wt % of glucose and 90 wt % of 1-butanol), and biphasic (2.5 wt % of glucose, 26 wt % of water, and 71.5 wt % of 1-butanol) mediums, without catalyst, were used in order to study the influence of those on HMF production from glucose. The glucose conversion and HMF yield data obtained in the mentioned process are summarized in Table 4. As it can be concluded, the use of a biphasic system provided a good glucose conversion and it improved HMF yield. In most of the cases, the presence of organic solvents in water (i) improves the dissolution of reactants,[29] (ii) facilitates the extraction of the desired or target products,[29] and (iii) prevents side reactions, such as rehydration and polymerization reactions to yield byproducts (levulinic acid, formic acid, and humins).[19,61]

After concluding that the presence of the 1-butanol improves the glucose conversion and HMF yield, the activity of ZrO_2 and γ-Al_2O_3 were tested using the biphasic reaction system and the same operation conditions. The obtained activity results are presented in Table 4.

Table 4. Glucose conversion and HMF yield obtained measured at 1.5 MPa of N_2 and 200 °C for 1.5 h for different reaction variables

Reaction variable	Reaction medium	Glucose conversion (%)	HMF yield (%)
Medium (without catalyst)	Aqueous	66.8	12.2
	Biphasic	82.8	14.3
	organic	90.7	1.9
Support (in biphasic medium)	Al_2O_3	96.8	5.9
	ZrO_2 cal	91.9	23.4
	$CuCr_2O_3$	95.9	11.7
Catalyst (in biphasic medium)	2.5CuZr	86.9	23.4
	10CuZr	75.8	25.6
	15CuZr	85.8	19.2
	20CuZr	81.9	19.0

Although both catalytic materials provide a high glucose conversion, the ZrO_2 support shows more capacity to transform glucose into the target product, the HMF. Probably, the acid nature of the Al_2O_3 support[11] could favor the presence of the acidic conditions, which are responsible for the side reactions

suffered from HMF. Yan et al.[62] tested ZrO_2 and ZrO_2−Al_2O_3 type solid catalysts, and they report that the catalyst with moderate acid and basic properties is more appropriate to favor the HMF formation using glucose as a raw material.

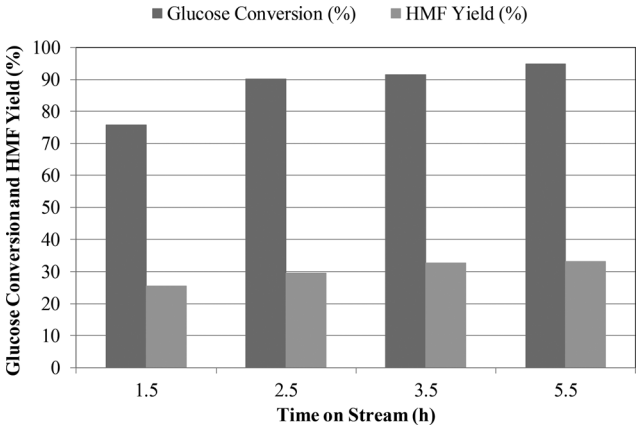

Figure 6. Evolution of glucose conversion and HMF yield with the reaction time for the 10CuZr catalyst obtained at 200 °C and 1.5 MPa of N_2.

Afterward, the ZrO_2 material was used as support of different quantities of Cu for its use in HMF production.

Different metal cations,[63,64] such as Cu^{2+}, can be used as modifiers of the acidic properties of supports. They can work as oxidation and hydrogenation catalysts, and they are applied to a wide range of reactions. Apart from CuZr catalysts, the commercial $CuCr_2O_3$ catalyst was also used in the dehydration reaction of glucose, in order to compare its activity with the CuZr ones. Table 4 shows the activity results obtained, indicating that the $CuCr_2O_3$ catalyst provided lower HMF yield than Zr-supported ones.

Although the Zr-supported Cu catalysts show a slightly lower glucose conversion than the ZrO_2 calcined support, some of them provide a higher HMF yield. The value of this last parameter changes with the Cu loading, reaching the highest HMF yield for the 10CuZr catalyst and the lowest glucose conversion. Meanwhile, the 2.5CuZr and 15CuZr catalysts provide higher glucose conversion and a HMF yield slightly lower than the obtained one by the 10CuZr catalyst. The 20CuZr catalyst presents the lowest glucose conversion and HMF yield. Marianou et al.[18] obtained similar HMF yields, between 2.5 and 25%, for glucose conversions around 60−100% under softer operating conditions using Sn oxide supported catalysts. They associated these low HMF yields to the existence of many active Lewis acid sites which are promoters of lactic acid, levulinic acid,[65] and other byproducts. The presented results in this work are in a good agreement with the Marioanoúsresults. The presence of low and moderated Lewis acid sites measured by TPD-NH_3 explains the low HMF yield obtained. All of the prepared Zr-supported Cu catalysts present low glucose conversion, which can be ascribed to the strength of the Lewis acid sites. Moreover, it seems that Bronsted acid sites coming from Zr species are necessary to increase the HMF yield. Shahangi et al.20 and Jiang et al.66 obtained HMF yields, above 34%, using silica-alumina and zirconium based catalyst at 170 °C and in biphasic-systems. In the last case, the good performance of the zirconium based catalyst was ascribed to the well dispersion of ZrO2 nanoparticles and the presence of multicoordinated Zr4+ species. In addition Xia et al.67 registered an HMF yield of 61% at 120 °C and 5 bar of pressure using a β-zeolite supported Fe catalyst; they associated this behavior to the synergetic effect between Lewis and Bronsted acid sites. According to the literature,29 low pore size catalysts facilitate the formation of platform molecules, hindering diffusion of raw material into the pores and therefore limiting side reactions. Although it seems to be a relationship between low pore size and HMF yield, in these cases, the possible correlation of textural data and HMF yield is a little bit weak because the difference of pore size values could be within the experimental error.

Taking into account the activity results for Cu-supported catalysts, the glucose dehydration was carried out for longer reaction times with the 10CuZr catalyst. As Figure 6 suggests, the conversion and HMF yield increases with the reaction time and reaches the stationary state and the optimum HMF yield after 3.5 h of reaction time. Concretely a 33% HMF yield is obtained for a 90% glucose conversion. At 5.5 h of reaction time the glucose conversion increased a little bit, but the HMF yield remained almost constant. Based on the data presented in Figure 6, the higher HMF after 3.5 h of reaction time. Concretely a 33% HMF yield is obtained for a 90% glucose conversion. At 5.5 h of reaction time the glucose conversion increased a little bit, but the HMF yield remained almost constant. Based on the data presented in Figure 6, the higher HMF yield is probably related with the higher glucose conversion.

3.2.2. DMF production

The same catalysts and Zr support used in glucose dehydration were employed for "high grade HMF" hydrogenolysis to produce DMF. In this process, a fixed bed reactor was used under the same temperature and pressure conditions as the glucose dehydration process. However, in this case, as a hydrogen donor is required for the hydro- genolysis reaction, H_2 was used instead of N_2. In most of the latest developments, the hydrogenolysis of HMF to produce DMF has been carried out in batch reactors, and few works are published using fixed bed reactors. For instance, in batch reactor systems some authors like Srivastava et al.[68] reached 78% of DMF selectivity and complete HMF conversion at 220 °C and 30 bar of hydrogen with a Cu−Co bimetallic catalyst supported on Al_2O_3. These researchers attribute the good catalytic performance to the presence of mixed copper−cobalt species on porous Al_2O_3. Li et al.[69] obtained 83.3% of DMF selectivity at complete HMF conversion using Co_3O_4 catalyst. They relate this high yield to the bifunctional behavior of the catalyst, where Co acts as the active site metal and CoO_x activates the C−O bonds as Lewis acid sites. Higher DMF yield (90%) was obtained by Yang et al. [70] using a bimetallic catalyst of Ni−Co supported on carbon with formic acid as hydrogen donor. The presence of Cu also activates the C−O bonds cleavage69,71−73 as Lewis acid sites, that is why in this work the copper catalysts present some DMF yield and the ZrO2 calcined support does not. The activity results reflected in Table 5 indicate that only the Zr-supported catalysts are able to convert completely HMF with considerable DMF yields.

Table 5. HMF conversion and DMF yield obtained for different ZrO_2 supported Cu catalyst at 1.5 MPa of H_2, 200 °C, and WHSV = 0.15 h^{-1} for 4h.

Catalyst	HMF conversion (%)	DMF yield (%)
ZrO_2 cal[a]	0.0	0.0
$CuCr_2O_3$	100.0	5.6
2.5CuZr	97.0	18.0
10CuZr	98.5	27.8
15CuZr	100.0	30.0
20CuZr	100.0	26.8
1Ru15CuZr	100.0	45.6

All the tested catalysts, except calcined ZrO2 support, are able to convert completely HMF. However, among Zr supported monometallic catalysts, the 15CuZr catalyst provides the best results for the DMF yield (30%) followed by 10CuZr, 20CuZr, and 2.5CuZr, respectively. Although the results among 10CuZr, 15CuZr, and 20CuZr catalysts were quite similar, probably due to their similar acidity (see Table 2) and

textural properties (see Table 1), the higher HMF yield can be related to the high copper amount on the catalytic surface of the 15CuZr catalysts (see Figure 7). There is a clear tendency between the Cu^0/Zr of the used catalyst and the DMF yield as it can be observed in Figure 7. The higher amount of metallic copper on the catalytic surface the higher DMF yield was reached. However, the sintering tendency and coke production are quite similar than in 10CuZr and 20CuZr catalysts. Based on these results, a small amount of Ru was added to the 15CuZr catalyst with the aim of improving the hydrogenation capacity of it. The presence of ruthenium on the 15CuZr catalyst improves the DMF yield from 30% to 45.6% (see Figure 7). It seems that the presence of the ruthenium not only improves the amount of copper on the catalytic surface but also seems to take part on the catalytic reaction (see Table 3 and XPS and CO chemisorption results, Figures S1 and S2, Table S1, and Figure 7 respectively). This is an important factor in the HMF yield as it can be observed in Figure 7. It seems to be a correlation between the obtained DMF yield in HMF hydrogenolysis and the surface properties measured by the XPS characterization technique.[74] According to the correlation presented in Figure 7, DMF yield increases with increasing the surface Cu^0/Zr ratio (associated metallic Cu on the surface) and decreasing the C/Zr ratio (ascribed to coke formation during hydrogenolysis reaction) for used catalyst (see Table 3). In this sense, the 15CuZr catalyst shows the highest DMF yield due to its higher Cu^0/Zr ratio and lower C/Zr ratio after its use in the reaction. The presence of Ru modifies the surface characteristics of 15CuZr catalyst, and it stabilizes the catalysts regarding the coke production. Moreover, as it can be observed in Figure 7, the ruthenium could also take part in the reaction, since the obtained DMF yield is higher than the corresponding one at the Cu^0/Zr ratio for used catalyst. With a Cu^0/Zr ratio of 0.072 the achieved DMF yield was 45%, while the monometallic 15Cu/Zr, with a higher Cu^0/Zr ratio for used catalyst, presents a lower DMF yield. The low tendency of the coke formation is related to the presence of little amounts of ruthenium on the catalysts, which also improves the metal reduction (see Figures 2 and 3) during the reaction (see Table 3). This fact improves the stability of the catalyst and limits the coke production; the minor presence of Cu_2O and CuO on the catalytic surface disfavors the coke formation (see Table 3) due to, as previously mentioned, the 1Ru15CuZr catalyst being the only catalyst that after being used in the reaction shows a higher $Cu^0/(Cu^+ + Cu^{2+})$ ratio.

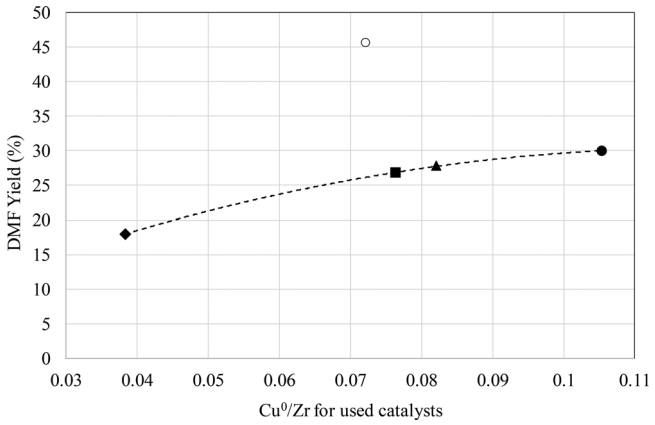

Figure 7. Correlation between DMF yield and Cu^0/Zr ratio measured by XPS technique for different used Zr-supported catalysts (◆ 2.5CuZr, ▲ 10 CuZr, ● 15CuZr, ■ 20 CuZr, ○ 1Ru15CuZr).

Thus, it improves the coke resistance, and it increases the amount of reduced species (related to the better reducibility when Ru is added) on the surface of the used 15CuZr catalyst, providing a better behavior toward DMF production.

Following the procedure employed in the glucose dehy- dration, influence of the time on stream was measured for the 1Ru15CuZr catalyst. The results presented in Figure 8 indicate that after 4.5 h the HMF conversion increases slightly, remaining almost constant during the following hours, while DMF yield decreases from 45.6% to 18%.

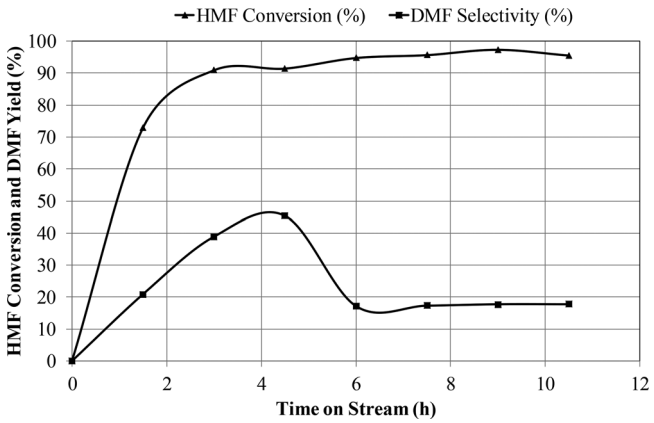

Figure 8. Evolution of HMF conversion and DMF yield with the time on stream for the 1Ru15CuZr catalyst at 200 °C, 1.5 MPa of H_2, and WHSV = 0.15 h^{-1}

The conversion and DMF yield keep constant after 6 h at values of 95% and 18%, respectively. Therefore, the presence of new products or byproduct is clear, even when the DMF yield is the highest one (45.6%). This behavior could be due to the loss of structural properties on the catalytic surface related to the decrease of Cu species and increase of C/Zr ratio as XPS results show.

Finally, after the optimization process of the HMF hydrogenolysis reaction to produce DMF, an activity test using "low grade HMF" (obtained from glucose dehydration process) was performed using the same operation conditions and the 1Ru15CuZr catalyst. The obtained results (see Figure 9) indicate that HMF conversion and DMF yield are lower than obtained ones with the synthetic HMF. Concretely, glucose derived HMF conversion is around 77%, while for "high grade HMF" conversion it is close to 91% after 4 h of time on stream. In the case of DMF yield, the difference is more pronounced, because DMF yield obtained for glucose derived HMF is 16.4%, while the DMF yield for "high grade HMF" is 45.6%. The low DMF yield obtained from "low grade HMF" conversion could be ascribed to the impurities associated with the used feed.[11]

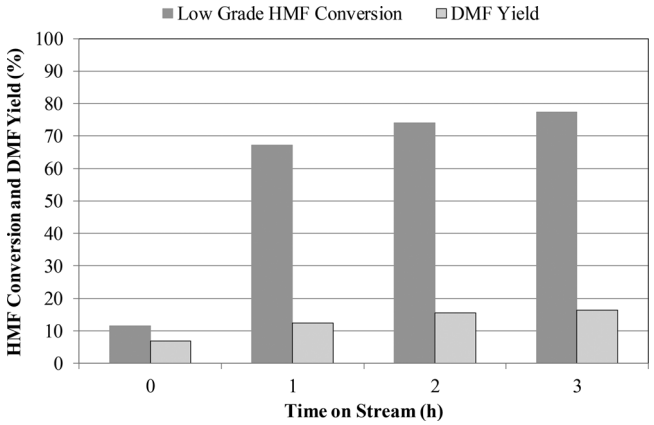

Figure 9. "Low grade HMF" conversion and DMF yield for the 1Ru15CuZr catalyst obtained at 200 °C, 1.5 MPa of H_2, WHSV = 0.15 h^{-1}, and 4 h of time on stream

4. Conclusions

The main goal of this work was to prepare metallic Cu catalysts supported on ZrO_2 material, which offers good characteristics for its use in DMF production through HMF hydrogenolysis. Moreover, these catalysts were also employed in glucose dehydration reactions to produce HMF. The hydrogenolysis reaction was carried out in a continuous fixed bed reactor, while glucose dehydration reactions were carried out in a discontinuous batch reactor. The same temperature, 200 °C, and pressure, 1.5 MPa, were selected for

both processes. However, to maintain the selected pressure different gases were used, concretely N_2 for dehydration and H_2 for hydrogenolysis.

With regards to the glucose dehydration, the results conclude that (i) glucose conversion and HMF yield are improved using biphasic systems. These kinds of systems enhance the dissolution of the raw material, the extraction of the target product, and, along with the presence of ZrO_2 neutral-basic support, hinder undesirable side reactions. (ii) Among the Zr-supported catalysts, the 10CuZr catalyst, the one which shows the lowest average pore size and adequate Lewis acid sites, provides the highest HMF yield (25.6%); and apart from Cu loading, longer reaction times have a positive influence on the conversion and HMF yield, reaching values of 90% and 33.5%, respectively, after 5.5 h, probably due to the higher glucose conversion.

In the case of DMF production, there seems to be a close relationship between DMF yield and surface characteristics measured by the XPS characterization technique. According to the results, among Zr-supported Cu catalysts, the 15CuZr catalyst shows the highest DMF yield (30%) due to the highest exposure of surface Cu species and the lowest formation of coke after reaction. In this sense, the presence of Ru in the 15CuZr catalyst also improves the coke resistant ability and increases the presence of more reduced Cu species on the surface, which seems to be related to the enhancement of the catalyst reducibility. In addition, it seems that the ruthenium also takes place in the DMF reaction due to the best result reached in the DMF yield. These good characteristics confer to the 1Ru15CuZr catalyst the capacity to produce more DMF, reaching a yield of 45.6% after 4 h of time on stream when "high grade HMF" is used. Finally, it is also concluded that the impurities presented in the "low grade HMF" could be the cause of the lower HMF conversion and DMF yield that were obtained.

Supporting information

The Supporting Information is available free of charge on the ACS Publications website at DOI: 10.1021/acs.iecr.8b01234.

Aknowledgments

This work was supported by the University of the Basque Country (UPV/EHU), the Spanish Ministry of Economy and Innovation and European Union through the European Regional Development Fund (FEDER) (Project: CTQ2015- 64226-C3-2-R), and the Basque Country Government (Project: IT993-16). The authors also express their gratitude to the Analysis General Services (SGIker) attached to the UPV/EHU University for its assistance with the TEM analysis.

References

(1) Nishimura, S.; Ikeda, N.; Ebitani, K. Selective Hydrogenation of Biomass-Derived 5-Hydroxymethylfurfural (HMF) to 2,5-Dimethyl- furan (DMF) under Atmospheric Hydrogen Pressure over Carbon Supported PdAu Bimetallic Catalyst. *Catal. Today* 2014, *232*, 89−98.

(2) Zu, Y.; Yang, P.; Wang, J.; Liu, X.; Ren, J.; Lu, G.; Wang, Y. Efficient Production of the Liquid Fuel 2,5-Dimethylfuran from 5- Hydroxymethylfurfural over Ru/Co3O4 Catalyst. *Appl. Catal., B* 2014, *146*, 244−248.

(3) International Energy Agency. *World Energy Outlook 2015*; Paris, 2015.

(4) International Energy Agency. *Key Oil Trends*; 2016.

(5) Zhang, M.; Tong, X.; Ma, R.; Li, Y. Catalytic Transformation of Carbohydrates into 5-Hydroxymethyl Furfural over Tin Phosphate in a Water-Containing System. *Catal. Today* 2016, *264*, 131−135.

(6) Yang, P.; Cui, Q.; Zu, Y.; Liu, X.; Lu, G.; Wang, Y. Catalytic Production of 2,5-Dimethylfuran from 5-Hydroxymethylfurfural over Ni/Co3O4 Catalyst. *Catal. Commun.* 2015, *66*, 55−59.

(7) De, S.; Saha, B.; Luque, R. Hydrodeoxygenation Processes: Advances on Catalytic Transformations of Biomass-Derived Platform Chemicals into Hydrocarbon Fuels. *Bioresour. Technol.* 2015, *178*, 108−118.

(8) Qian, Y.; Zhu, L.; Wang, Y.; Lu, X. Recent Progress in the Development of Biofuel 2,5-Dimethylfuran.

Renewable Sustainable Energy Rev. 2015, *41*, 633−646.
(9) Green Chemistry. *Fraunhofer Magazine 2.2012*; 2012.
(10) Rosatella, A. A.; Simeonov, S. P.; Frade, R. F. M.; Afonso, C. A.
M. 5-Hydroxymethylfurfural (HMF) as a Building Block Platform: Biological Properties, Synthesis and Synthetic Applications. *Green Chem.* 2011, *13* (4), 754−793.
(11) Iriondo, A.; Mendiguren, A.; Güemez, M. B.; Requies, J.;
Cambra, J. F. 2,5-DMF Production through Hydrogenation of Real and Synthetic 5-HMF over Transition Metal Catalysts Supported on Carriers with Different Nature. *Catal. Today* 2017, *279* (2), 286−295.
(12) Menon, V.; Rao, M. Trends in Bioconversion of Lignocellulose: Biofuels, Platform Chemicals & Biorefinery Concept. *Prog. Energy Combust. Sci.* 2012, *38* (4), 522−550.
(13) Climent, M. J.; Corma, A.; Iborra, S. Conversion of Biomass Platform Molecules into Fuel Additives and Liquid Hydrocarbon Fuels. *Green Chem.* 2014, *16* (2), 516−547.
(14) Choi, S.; Song, C. W.; Shin, J. H.; Lee, S. Y. Biorefineries for the Production of Top Building Block Chemicals and Their Derivatives. *Metab. Eng.* 2015, *28*, 223−239.
(15) Zhang, Y.; Zhang, J.; Su, D. 5-Hydroxymethylfurfural: Akey Intermediate for Efficient Biomass Conversion. *J. Energy Chem.* 2015, *24* (5), 548−551.
(16) Roman-Leshkov, Y.; Barrett, C. J.; Liu, Z. Y.; Dumesic, J. A. Production of Dimethylfuran for Liquid Fuels from Biomass-Derived Carbohydrates. *Nature* 2007, *447* (7147), 982−985.
(17) Zhao, J.; Zhou, C.; He, C.; Dai, Y.; Jia, X.; Yang, Y. Efficient Dehydration of Fructose to 5-Hydroxymethylfurfural over Sulfonated Carbon Sphere Solid Acid Catalysts. *Catal. Today* 2016, *264*, 123−130.
(18) Marianou, A. A.; Michailof, C. M.; Pineda, A.; Iliopoulou, E. F.; Triantafyllidis, K. S.; Lappas, A. A. Effect of Lewis and BrØnsted Acidity on Glucose Conversion to 5-HMF and Lactic Acid in Aqueous and Organic Media. *Appl. Catal., A* 2018, *555* (November 2017), 75−87.
(19) Parveen, F.; Upadhyayula, S. Efficient Conversion of Glucose to HMF Using Organocatalysts with Dual Acidic and Basic Function- alities - A Mechanistic and Experimental Study. *Fuel Process. Technol.* 2017, *162*, 30−36.
(20) Shahangi, F.; Najafi Chermahini, A.; Saraji, M. Dehydration of Fructose and Glucose to 5-Hydroxymethylfurfural over Al-KCC-1 Silica. *J. Energy Chem.* 2018, *27* (3), 769−780.
(21) Toftgaard Pedersen, A.; Ringborg, R.; Grotkjær, T.; Pedersen, S.; Woodley, J. M. Synthesis of 5-Hydroxymethylfurfural (HMF) by Acid Catalyzed Dehydration of Glucose-Fructose Mixtures. *Chem. Eng. J.* 2015, *273*, 455−464.
(22) Shi, J.; Wang, Y.; Yu, X.; Du, W.; Hou, Z. Production of 2,5- Dimethylfuran from 5-Hydroxymethylfurfural over Reduced Gra- phene Oxides Supported Pt Catalyst under Mild Conditions. *Fuel* 2016, *163*, 74−79.
(23) Xu, N.; Wu, Y.; Tang, C.; Zhang, P.; He, X.; Wang, Z.; Huang,
Z. Experimental Study of 2,5-Dimethylfuran and 2-Methylfuran in a Rapid Compression Machine: Comparison of the Ignition Delay Times and Reactivity at Low to Intermediate Temperature. *Combust. Flame* 2016, *168*, 216−227.
(24) Jęża̧k, S.; Dzida, M.; Zorębski, M. High Pressure Physicochem- ical Properties of 2-Methylfuran and 2,5-Dimethylfuran − Second Generation Biofuels. *Fuel* 2016, *184*, 334−343.
(25) Conturso, M.; Sirignano, M.; D'Anna, A. Effect of 2,5-
Dimethylfuran Doping on Particle Size Distributions Measured in Premixed Ethylene/Air Flames. *Proc. Combust. Inst.* 2017, *36* (1),
985−992.
(26) Chatterjee, M.; Ishizaka, T.; Kawanami, H. Hydrogenation of 5- Hydroxymethylfurfural in Supercritical Carbon Dioxide-Water: A Tunable Approach to Dimethylfuran Selectivity. *Green Chem.* 2014, *16* (3), 1543−1551.
(27) Srivastava, S.; Jadeja, G. C.; Parikh, J. Synergism Studies on Alumina-Supported Copper-Nickel

Catalysts towards Furfural and 5- Hydroxymethylfurfural Hydrogenation. *J. Mol. Catal. A: Chem.* 2017, *426*, 244−256.
(28) Tang, X.; Wei, J.; Ding, N.; Sun, Y.; Zeng, X.; Hu, L.; Liu, S.; Lei, T.; Lin, L. Chemoselective Hydrogenation of Biomass Derived 5- Hydroxymethylfurfural to Diols: Key Intermediates for Sustainable Chemicals, Materials and Fuels. *Renewable Sustainable Energy Rev.* 2017, *77* (July2016), 287−296.
(29) Requies, J.; Agirre, I.; Iriondo, A. Production of Furanic Biofuels with Zeolite and Metal Oxide Bifunctional Catalysts for Energy- and Product-Driven Biorefineries. In *Production of Biofuels and Chemicals with Bifunctional Catalysts*; Fang, Z., Smith, R. L., Jr., Li, H., Eds.; Springer: Singapore, 2017; pp 239−271.
(30) Topsøe, N.-Y.; Pedersen, K.; Derouane, E. G. Infrared and Temperature-Programmed Desorption Study of the Acidic Properties of ZSM-5-Type Zeolites. *J. Catal.* 1981, *70* (1), 41−52.
(31) Wang, G.-H.; Hilgert, J.; Richter, F. H.; Wang, F.; Bongard, H.- J.; Spliethoff, B.; Weidenthaler, C.; Schüth, F. Platinum−cobalt Bimetallic Nanoparticles in Hollow Carbon Nanospheres for Hydrogenolysis of 5-Hydroxymethylfurfural. *Nat. Mater.* 2014, *13* (3), 293−300.
(32) Nagpure, A. S.; Lucas, N.; Chilukuri, S. V. Efficient Preparation of Liquid Fuel 2,5-Dimethylfuran from Biomass-Derived 5-Hydrox- ymethylfurfural over Ru−NaY Catalyst. *ACS Sustainable Chem. Eng.* 2015, *3* (11), 2909−2916.
(33) Luo, J.; Lee, J. D.; Yun, H.; Wang, C.; Monai, M.; Murray, C. B.; Fornasiero, P.; Gorte, R. J. Base Metal-Pt Alloys: A General Route to High Selectivity and Stability in the Production of Biofuels from HMF. *Appl. Catal., B* 2016, *199*, 439−446.
(34) Chen, B.; Li, F.; Huang, Z.; Yuan, G. Carbon-Coated Cu-Co Bimetallic Nanoparticles as Selective and Recyclable Catalysts for Production of Biofuel 2,5-Dimethylfuran. *Appl. Catal., B* 2017, *200*, 192−199.
(35) Goyal, R.; Sarkar, B.; Bag, A.; Siddiqui, N.; Dumbre, D.; Lucas, N.; Bhargava, S. K.; Bordoloi, A. Studies of Synergy between Metal− support Interfaces and Selective Hydrogenation of HMF to DMF in Water. *J. Catal.* 2016, *340*, 248−260.
(36) Upare, P. P.; Hwang, D. W.; Hwang, Y. K.; Lee, U.-H.; Hong, D.-Y.; Chang, J.-S. An Integrated Process for the Production of 2,5- Dimethylfuran from Fructose. *Green Chem.* 2015, *17* (6), 3310−3313.
(37) Bhanja, P.; Bhaumik, A. Porous Nanomaterials as Green Catalyst for the Conversion of Biomass to Bioenergy. *Fuel* 2016, *185*, 432−441.
(38) Seo, Y. S.; Jung, Y. S.; Yoon, W. L.; Jang, I. G.; Lee, T. W. The Effect of Ni Content on a Highly Active Ni-Al2O3 Catalyst Prepared by the Homogeneous Precipitation Method. *Int. J. Hydrogen Energy* 2011, *36* (1), 94−102.
(39) El Doukkali, M.; Iriondo, A.; Miletic, N.; Cambra, J. F.; Arias,
P. L. Hydrothermal Stability Improvement of NiPt-Containing γ-Al 2 O 3 Catalysts Tested in Aqueous Phase Reforming of Glycerol/Water Mixture for H 2 Production. *Int. J. Hydrogen Energy* 2017, *42* (37), 23617−23630.
(40) Sagar, G. V.; Venkat, P.; Rao, R.; Srikanth, C. S.; Chary, K. V.
R. Dispersion and Reactivity of Copper Catalysts Supported on Al2O3 -ZrO2. *J. Phys. Chem. B* 2006, *110* (28), 13881−13888.
(41) López, P.; Mondragón-Galicia, G.; Espinosa-Pesqueira, M. E.; Mendoza-Anaya, D.; Fernández, M. E.; Gómez-Cortés, A.; Bonifacio, J.; Martínez-Barrera, G.; Pérez-Hernández, R. Hydrogen Production
from Oxidative Steam Reforming of Methanol: Effect of the Cu and Ni Impregnation on ZrO2 and Their Molecular Simulation Studies. *Int. J. Hydrogen Energy* 2012, *37* (11), 9018−9027.
(42) Aguila, G.; Valenzuela, A.; Guerrero, S.; Araya, P. WGS Activity of a Novel Cu-ZrO2 Catalyst Prepared by a Reflux Method. Comparison with a Conventional Impregnation Method. *Catal. Commun.* 2013, *39*, 82−85.
(43) Águila, G.; Gracia, F.; Cortés, J.; Araya, P. Effect of Copper
Species and the Presence of Reaction Products on the Activity of Methane Oxidation on Supported CuO Catalysts. *Appl. Catal., B* 2008, *77* (3−4), 325−338.

(44) Freitas, I. C.; Damyanova, S.; Oliveira, D. C.; Marques, C. M. P.; Bueno, J. M. C. Effect of Cu Content on the Surface and Catalytic Properties of Cu/ZrO 2 Catalyst for Ethanol Dehydrogenation. *J. Mol. Catal. A: Chem.* 2014, *381*, 26−37.

(45) Ding, J.; Liu, Y.; Zhang, J.; Dong, M.; Wang, Y.; He, W.; Han, X.; Liu, K.; Jiang, Z.; Chen, J. Synergism from Interfaces between Cu and Crystalline ZrO2nanosheets Fabricated by Acetic Complex Method for Oxalates Hydrogenation. *Mol. Catal.* 2017, *438*, 93−102.

(46) Soares, A. V. H.; Salazar, J. B.; Falcone, D. D.; Vasconcellos, F. A.; Davis, R. J.; Passos, F. B. A Study of Glycerol Hydrogenolysis over Ru-Cu/Al2O3 and Ru-Cu/ZrO2 Catalysts. *J. Mol. Catal. A: Chem.* 2016, *415*, 27−36.

(47) Salazar, J. B.; Falcone, D. D.; Pham, H. N.; Datye, A. K.; Passos,
F. B.; Davis, R. J. Selective Production of 1,2-Propanediol by Hydrogenolysis of Glycerol over Bimetallic Ru-Cu Nanoparticles Supported on TiO2. *Appl. Catal., A* 2014, *482*, 137−144.

(48) Iriondo, A.; Cambra, J. F. F.; Barrio, V. L. L.; Guemez, M. B. B.; Arias, P. L. L.; Sanchez-Sanchez, M. C. C.; Navarro, R. M. M.; Fierro,J. L. G. L. G. Glycerol Liquid Phase Conversion over Monometallic and Bimetallic Catalysts: Effect of Metal, Support Type and Reaction Temperatures. *Appl. Catal., B* 2011, *106* (1−2), 83−93.

(49) Li, D.; Nakagawa, Y.; Tomishige, K. Methane Reforming to Synthesis Gas over Ni Catalysts Modified with Noble Metals. *Appl. Catal., A* 2011, *408* (1−2), 1−24.

(50) Requies, J.; Güemez, M. B.; Iriondo, A.; Barrio, V. L.; Cambra, J. F.; Arias, P. L. Bio N-Butanol Partial Oxidation to Butyraldehyde in Gas Phase on Supported Ru and Cu Catalysts. *Catal. Lett.* 2012, *142* (4), 417−426.

(51) Fatimah, I.; Rubiyanto, D.; Kartika, N. C. Effect of Calcination Temperature on the Synthesis of ZrO < inf > 2</Inf>-Pillared Saponite to Catalytic Activity in Menthol Esterification. *Indones. J. Chem.* 2016, *16* (1), 8−13.

(52) Kochkin, Y. N.; Vlasenko, N. V.; Struzhko, V. L.; Puziy, A. M.; Strizhak, P. E. Methanol Carboxylation over Zirconium Dioxide: Effect of Catalyst Phase Composition on Its Acid-Base Spectrum and Direction of Catalytic Transformations. *Can. J. Chem. Eng.* 2016, *94* (4), 745−751.

(53) Khaodee, W.; Jongsomjit, B.; Praserthdam, P.; Goto, S.; Assabumrungrat, S. Impact of Temperature Ramping Rate during Calcination on Characteristics of Nano-ZrO2and Its Catalytic Activity for Isosynthesis. *J. Mol. Catal. A: Chem.* 2008, *280* (1−2), 35−42.

(54) Patankar, S. C.; Yadav, G. D. Cascade Engineered Synthesis of ??-Valerolactone, 1,4-Pentanediol, and 2-Methyltetrahydrofuran from Levulinic Acid Using Pd-Cu/ZrO2Catalyst in Water as Solvent. *ACS Sustainable Chem. Eng.* 2015, *3* (11), 2619−2630.

(55) Chary, K. V. R.; Seela, K. K.; Naresh, D.; Ramakanth, P. Characterization and Reductive Amination of Cyclohexanol and Cyclohexanone over Cu/ZrO2 Catalysts. *Catal. Commun.* 2008, *9* (1), 75−81

(56) Lee, H. J.; Kang, D. C.; Pyen, S. H.; Shin, M.; Suh, Y. W.; Han, H.; Shin, C. H. Production of H2-Free CO by Decomposition of Formic Acid over ZrO2catalysts. *Appl. Catal., A* 2017, *531*, 13−20.

(57) Pawelec, B.; Damyanova, S.; Arishtirova, K.; Fierro, J. L. G.; Petrov, L. Structural and Surface Features of PtNi Catalysts for Reforming of Methane with CO2. *Appl. Catal., A* 2007, *323*, 188− 201.

(58) Moulder, J. F.; Stickle, W. F.; Sobol, P. E.; Bomben, K. D. *Handbook of X-Ray Photoelectron Spectroscopy: A Reference Book of Standard Spectra for Identification and Interpretation of XPS Data*; Chastain, J., Ed.; Perkin-Elmer Corporation Physical Electronics Division: 6509 Flying Cloud Drive, Eden Prairie, Minnosota 55344, United States of America, 1992.

(59) Hou, Z.; Yashima, T. Small Amounts of Rh-Promoted Ni Catalysts for Methane Reforming with CO2. *Catal. Lett.* 2003, *89* (3− 4), 193−197.

(60) Kaynar, A. D. D.; Dogu, D.; Yasyerli, N. Hydrogen Production and Coke Minimization through Reforming of Kerosene over Bi- Metallic Ceria-Alumina Supported Ru-Ni Catalysts. *Fuel Process. Technol.* 2015, *140*, 96−103

(61) Yu, I. K. M.; Tsang, D. C. W. Conversion of Biomass to Hydroxymethylfurfural: A Review of Catalytic

Systems and Under- lying Mechanisms. *Bioresour. Technol.* 2017, *238*, 716−732.

(62) Yan, H.; Yang, Y.; Tong, D.; Xiang, X.; Hu, C. Catalytic Conversion of Glucose to 5-Hydroxymethylfurfural over SO42-/ZrO2 and SO42-/ZrO2-Al2O3 Solid Acid Catalysts. *Catal. Commun.* 2009, *10* (11), 1558−1563.

(63) Agarwal, B.; Kailasam, K.; Sangwan, R. S.; Elumalai, S. Traversing the History of Solid Catalysts for Heterogeneous Synthesis of 5-Hy26droxymethylfurfural from Carbohydrate Sugars: A Review. *Renewable Sustainable Energy Rev.* 2018, *82*, 2408−2425.

(64) Hara, M.; Nakajima, K.; Kamata, K. Recent Progress in the Development of Solid Catalysts for Biomass Conversion into High Value-Added Chemicals. *Sci. Technol. Adv. Mater.* 2015, *16* (3), 034903 (22 pp).

(65) Wei, W.; Wu, S. Experimental and Kinetic Study of Glucose Conversion to Levulinic Acid in Aqueous Medium over Cr/HZSM-5 Catalyst. *Fuel* 2018, *225* (April), 311−321.

(66) Jiang, C.; Zhu, J.; Wang, B.; Li, L.; Zhong, H. One-Pot Synthesis of 5-Hydroxymethylfurfural from Glucose over Zirconium Dopped Mesoporous KIT-6. *Chin. J. Chem Eng.* 2018, 26 (6), 1270-1277.

(67) Xia, H.; Hu, H.; Xu, S.; Xiao, K.; Zuo, S. Catalytic Conversion of Glucose to 5-Hydroxymethyfural over Fe/B Zeolites with Extra- Framework Isolated Fe Species in a Biphasic Reaction System. *Biomass Bioenergy* 2018, *108* (June 2017), 426−432.

(68) Srivastava, S.; Jadeja, G. C.; Parikh, J. Influence of Supports for Selective Production of 2, 5-Dimethylfuran via Bimetallic Copper -Cobalt Catalyzed 5-Hydroxymethylfurfural Hydrogenolysis. *Chin. J. Catal.* 2017, *38* (4), 699−709.

(69) Li, D.; Liu, Q.; Zhu, C.; Wang, H.; Cui, C.; Wang, C.; Ma, L. Selective Hydrogenolysis of 5-Hydroxymethylfurfural to 2,5-Dime- thylfuran over Co3O4catalyst by Controlled Reduction. *J. Energy Chem.* 2018, 1−8.

(70) Yang, P.; Xia, Q.; Liu, X.; Wang, Y. Catalytic Transfer Hydrogenation/Hydrogenolysis of 5-Hydroxymethylfurfural to 2,5- Dimethylfuran over Ni-Co/C Catalyst. *Fuel* 2017, *187*, 159−166.

(71) Sato, S.; Akiyama, M.; Takahashi, R.; Hara, T.; Inui, K.; Yokota, M. Vapor-Phase Reaction of Polyols over Copper Catalysts. *Appl. Catal., A* 2008, *347* (2), 186−191.Vasiliadou, E. S.;

(72) Lemonidou, A. A. Kinetic Study of Liquid- Phase Glycerol Hydrogenolysis over Cu/SiO2 Catalyst. *Chem. Eng. J.* 2013, *231*, 103−112.

(73) Rajkhowa, T.; Marin, G. B.; Thybaut, J. W. A Comprehensive Kinetic Model for Cu Catalyzed Liquid Phase Glycerol Hydro- genolysis. *Appl. Catal., B* 2017, *205*, 469−480.

(74) Tomishige, K.; Nakagawa, Y.; Tamura, M. Selective Hydro- genolysis of C−O Bonds Using the Interaction of the Catalyst Surface and OH Groups. In *Selective Catalysis for Renewable Feedstocks and Chemicals*; Nicholas, K. M., Ed.; Springer International Publishing: Cham, 2014; pp 127−162.